Journal of Molecular Structure 1294 (2023) 136495

Contents lists available at ScienceDirect

Journal of Molecular Structure

journal homepage: www.elsevier.com/locate/molstr

Calculation of the Raman frequencies and thermodynamic quantities at high pressures for the cubic gauche nitrogen (cg-N)

Hamit Yurtseven [a,*], Ozge Akay Sefer [b]

[a] Department of Computer Engineering, Baskent University, Ankara 06790, Turkey
[b] Department of Mechatronics Engineering, Marmara University, Istanbul 34854, Turkey

ARTICLE INFO

Keywords:
Raman frequencies
Mode Grüneisen parameter
υ-P relation
Thermodynamic quantities
cg-N structure

ABSTRACT

This study gives the calculation of the frequencies from the V-P Vinet EOS which has been modified as the frequency-pressure (υ-P) relation for the spectroscopic parameters in the cubic gauche nitrogen(cg-N). Calculation of the Raman frequencies is performed by means of the mode Grüneisen parameter as a function of pressure for the cg-N phase. From the Raman frequencies calculated, the pressure dependence of the thermodynamic quantities such as the free energy, entropy, heat capacity and the enthalpy are predicted by using the quasi-harmonic approximation for the cg-N structure.

Our results show that the υ-P relation derived from the V-P relation (Vinet-EOS) can be used to predict the frequencies and that the quasi-harmonic approximation is satisfactory to predict the thermodynamic quantities of interest, as exemplified for the cg-N structure in this study.

1. Introduction

Polymeric solid nitrogen has been attractive to study due to its potential application as a high energy density material. At high pressure, solid nitrogen can transform to an atomic solid with a single-bonded crystalline structure as predicted by McMahan and LeSar [1] and the covalent polymeric lattice has been considered by Mailhiot et al. [2] as the cubic gauche (cg-N) structure. This structure has been discovered experimentally by Eremets et al. under the temperature and pressure conditions of 2000 K and 110 GPa [3–5]. Fig. 1 gives the crystal structure of the cg-N [3]. For the stability of the cg-N at high pressures, some earlier works have been reported [6–8]. Theoretically, after Refs. [1,2], a large number of studies for the single-bonded nitrogen (cg-N) have been performed [9–16]. In particular, the solid polymerized nitrogen has been modelled [10]. First principles calculations have been conducted for the single-bonded cubic phase of nitrogen(cg-N) [11–17]. By using equations of the state, the phase transition parameters have been evaluated for the cg-N structure [18]. Recently, we have also studied the thermodynamic [19], vibrational, elastic and dielectric properties [20] of cubic gauche nitrogen (cg-N).

The nonmolecular solid phase of nitrogen which is metastable at the ambient pressure [21,22], occurs from the triple molecular bond of nitrogen at high pressures with the occurrence of the cg-N structure [2],as also indicated previously [12]. This occurrence of the polymeric form (cg-N) is due to the triple N≡N bond transformed into the single N—N bonds under high pressures [1,2,8]. It has been pointed out that the transformation of the diatomic phase into the single-bonded (polymeric) phase is of a first order transition with a volume change of 22% on the basis of the experimental measurements [4]. This volume jump with the P-T relationship including the latent heat and entropy during the transition from molecular to polymeric cg solid phases, has been calculated [18].

Regarding vibrational modes of the cg-N structure, there are four atoms in the primitive cell of cg-N. Amongst 12 vibrational modes, there are 3 acoustic modes and 9 optical modes. These are zone-centre modes. For the 3 acoustic modes, there exist one LA and two degenerate TA. Considering 9 optical modes, there are 1 triply degenerate, 2 doubly degenerate and 2 nondegenerate modes. These are all Raman active modes and 1 triply degenerate modes is also infrared active as also indicated previously [12]. However, it has been optical reported in an earlier study [7]. 9 zone-centre optical modes have been identified as 2 triply degenerate modes, 1 doubly degenerate and one nondegenerate mode for the cg-N structure. This has also been indicated that the 12 optical modes in the zone centre of the cubic gauche structure decompose as $A + E + 2T$ where the T modes are both Raman and infrared active and, the A and E modes are only Raman active [13].

* Corresponding author.
E-mail address: hamit@metu.edu.tr (H. Yurtseven).

https://doi.org/10.1016/j.molstruc.2023.136495
Received 22 May 2023; Received in revised form 31 July 2023; Accepted 25 August 2023
Available online 26 August 2023

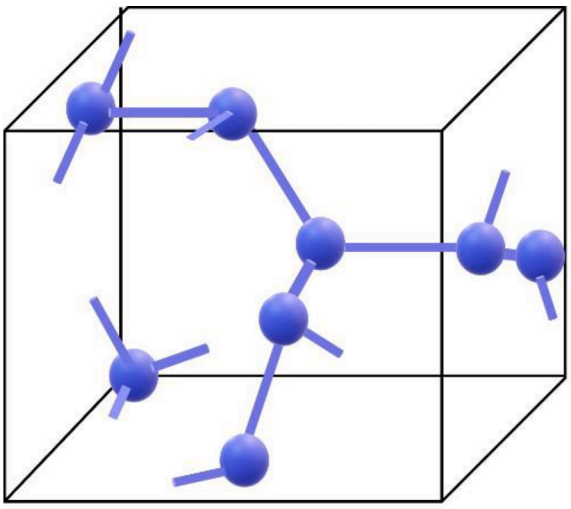

Fig. 1. Crystal structure of cg-N which was taken from Eremest et al. [3].

As stated above, using density functional theory (DFT) frequencies (Raman and infrared) of zone-centre phonon modes in cubic gauche nitrogen have been calculated as a function of pressure [7,13,16]. Experimentally, Raman frequencies of the 600 cm^{-1} (at $P = 0$) mode in comparison with the calculated [7] zone-centre phonon modes for the cg-N, were measured below 150 GPa [3,23]. Additionally, measurements of the Raman frequencies of ~800 cm^{-1} mode within the pressure region of 80-170 GPa for the cg-N structure have been reported [24,25]. The two low-frequency ~ 600 cm^{-1} and T (~ 800 cm^{-1}) modes are the lattice modes which are directly related to the polymeric chains. As explained previously [13], the A mode is the breathing mode of the cavities due to polymeric chains and the low-frequency T mode occurs which splits into the T(TO) and T(LO) (there also occurs the high frequency T(LO) mode as a vibron) due to the tilting of the N—N bonds relative to the direction of the polymeric chains.

Changes in the volume for the cg-N transition can be directly related to the frequency shifts by means of the mode Grüneisen parameter ɣ. Thus, the temperature and pressure dependence of the frequency can be predicted from those changes in the volume by the mode Grüneisen parameter in the polymeric form of nitrogen (cg-N). In our previous study for the cg-N structure [20], we have calculated the frequencies of the Raman and infrared optic modes of A, E, T(TO) and T(LO) as a function of pressure ($0 < P < 140$ GPa). Apart from the A and T modes as we defined, the E(~1000 cm^{-1}) mode occurs due to vibrations of the atoms parallel to (001), as noted in a previous study [13]. Using the observed V-P data and determining the pressure dependence of the isothermal mode Grüneisen parameter ($ɣ_T$), frequencies of those modes have been evaluated [20].

In the present study, we analyse the T modes, T(TO) and T(LO), ~ 800 cm^{-1} which are both Raman and infrared active and the A (~ 600 cm^{-1}) mode which is only Raman active [13]. Using the observed frequencies of the ~ 600 cm^{-1} [3] and ~ 800 cm^{-1} [24,25] modes, and the experimental V-P data [5] which were analysed according to the Vinet EOS [26], the pressure dependence of the isothermal mode Grüneisen parameter $ɣ_T$ for the A and T modes is determined for the cg-N structure. From this dependence, the frequencies of those modes are evaluated at various pressures ($T = 295$ K) for the cg-N phase. Using the frequencies calculated, the thermodynamic quantities of the free energy, entropy, heat capacity and the enthalpy are predicted as a function of pressure by using the quasi-harmonic theory. This theory has been modified for the spectroscopic parameters for the cg-N structure.

Below, we give an outline of the theory for the calculations, which is given in Section 2. Section 3 gives our calculations and results. They are discussed in Section 4. Finally, conclusions are given in Section 5.

2. Theory

Vibrational contributions to the thermodynamic properties can be investigated by the quasi-harmonic approximation [12,13,27,28]. In particular, the thermodynamical properties in the quasi- harmonic approximation have been computed for the cubic gauche nitrogen (cg-N) by integrating the phonon density of states over the whole frequency range [12,13,28]. With the quasi-harmonic contributions and the anharmonic corrections to the free energy, solid polymerized nitrogen [10] and the cubic gauche-polymeric phase of nitrogen(cg-N) [18] have been studied theoretically.

2.1. Quasi-harmonic (QH) theory

Within the quasi-harmonic approximation, the vibrational free energy is given by

$$F_{vib} = \frac{1}{2}\sum_i h\upsilon_i + k_B T \sum_i ln[1 - \exp(-h\upsilon_i / k_B T)] \tag{2.1}$$

with the Planck constant h and the Boltzmann constant k_B, where the first term is the zero point energy with the phonon modes i and the second term is the isothermal energy. By taking the derivative of the F_{vib} with respect to the temperature, we find the entropy S due to the vibrational modes as given by

$$S(T) = k_B \sum_i \frac{h\upsilon_i / k_B T}{\exp(h\upsilon_i / k_B T)} - k_B \sum_i ln[1 - \exp(-h\upsilon_i / k_B T)] \tag{2.2}$$

Using the definition of the heat capacity C_V (at constant volume), $C_V = T(\partial S/\partial T)_V$, the temperature dependence of the C_V is obtained as

$$C_v(T) = k_B \sum_i \left(\frac{h\upsilon_i}{k_B T}\right)^2 \frac{\exp(h\upsilon_i / k_B T)}{[\exp(h\upsilon_i / k_B T) - 1]^2} \tag{2.3}$$

which also gives the enthalpy H(T) from the definition $C_v = (\partial H/\partial T)_v$ as

$$H(T) = \frac{1}{2}\sum_i h\upsilon_i + \sum_i \frac{h\upsilon_i}{[\exp(h\upsilon_i / k_B T) - 1]} \tag{2.4}$$

As in the entropy S (Eqs. (2.2)–(2.4)) represent the contributions to the heat capacity and enthalpy,respectively, due to the vibrational modes. The above relations have been used to calculate F(T), S(T), C_v(T) and the enthalpy H(T) by means of the phonon density of states for the cg-N [12] and recently for the chalcopyrite-type compound $AgGaS_2$ [29]. Very recently, we have also used those relations within the quasi-harmonic approximation to calculate vibrational heat capacity, entropy and free energy due to Raman frequencies of the vibrational modes for hydrocarbons (solid benzene, naphthalene and antracene) [30]. Thus, by means of Eqs. (2.1)–(2.4) the temperature (and pressure) dependence of those thermodynamic quantities can be evaluated from the vibrational frequencies of modes at various temperatures and pressures in crystalline systems, in particular,for the cg-N, as studied here.

2.2. Calculation of the vibrational frequencies: mode Grüneisen parameter

The vibrational frequencies of various modes can be evaluated from the volume in general, by defining the mode Grüneisen parameter

$$\gamma_i = -\frac{V}{\upsilon_i}\left(\frac{d\upsilon_i}{dV}\right) \tag{2.5}$$

for the i th mode with the volume V of the crystalline system which has anharmonic properties. From this general definition of the mode Grüneisen parameters, we can also define the isobaric mode Grüneisen parameter ($ɣ_P$) for the i th vibrational mode by taking the derivatives of υ_i and V with respect to the temperature $(\partial\upsilon_i/\partial T)_p$ and $(\partial V/\partial T)_p$,

respectively. Similarly, the isothermal mode Grüneisen parameter γ_T can be defined by the derivatives $(\partial v_i/\partial P)_T$ and $(\partial V/\partial P)_T$ in Eq. (2.5). We have also introduced the mode Grüneisen parameter, in particular, the isothermal mode Grüneisen parameter γ_T to calculate the pressure dependence of the vibrational frequencies from the volume for the cubic gauche nitrogen (cg-N) in our recent study [20].

Regarding the calculation of the vibrational frequency v from the volume through the mode Grüneisen parameter, Eq. (2.5) can be solved for the v_i and in the case of the pressure dependence of the vibrational frequency, one can obtain

$$v(P) = v_0 \exp\left[-\gamma_T ln\frac{V(P)}{V_0}\right] \tag{2.6}$$

where v_0 and V_0 represent the vibrational frequency and the volume, respectively, at zero pressure ($P = 0$) and room temperature ($T = 295$ K).

For the calculation of the volume as a function of the pressure through which the vibrational frequencies can be evaluated by means of the γ_T in Eq. (2.6), we can employ the Vinet equation of state (EOS) as

$$P = 3B_0\left(\frac{1-f_v}{f_v^2}\right)exp\left[\frac{3}{2}(C_0-1)(1-f_v)\right] \tag{2.7}$$

where

$$f_v = (V/V_0)^{1/3} \tag{2.8}$$

In Eq. (2.8), V_0 denotes the cell volume at ambient pressure($P = 0$). B_0 and C_0 are the isothermal bulk modulus and its derivative against pressure at $P = 0$, respectively [26].

2.3. Modification of the Vinet EOS for the spectroscopic parameters

The Vinet EOS (Eq. (2.7)) can be modified by means of the mode Grüneisen parameter (Eq. (2.5)) for the vibrational frequency shifts $(\partial v_i/\partial P)_T$ in a crystalline system. Thus, the volume-pressure (V-P) relation in the Vinet EOS can be correspondingly expressed as the frequency-pressure (v-P) relation for the spectroscopic parameters. The functional form f_v as the ratio of the volume (Eq. (2.8)) in the Vinet EOS (Eq. (2.7)), can be expressed in terms of the ratio of the frequency by using Eq. (2.6) as

$$u_v = (v/v_0)^{-\frac{1}{3\gamma_T}} \tag{2.9}$$

This gives the (v-P) dependence of the f_v as the V-P dependence in the Vinet EOS (Eq. (2.7)). The other coefficients B_0 the isothermal bulk modulus and its derivative against pressure C_0 at $P = 0$ in Eq. (2.7), can be also defined spectroscopically by using the definition of the isothermal mode Grüneisen parameter γ_T according to Eq. (2.5),

$$\gamma_T(P) = -\frac{V(P)}{v(P)}\frac{(\partial v/\partial P)_T}{(\partial V/\partial P)_T} \tag{2.10}$$

From the definition of the bulk modulus $B = -V(P)(\partial P/\partial V)_T$ at zero pressure ($P = 0$),B_0 is defined through Eq. (2.10) as

$$B_0 = \gamma_T(P)v(P)(\partial P/\partial v)_T \tag{2.11}$$

In this expression, the frequency shifts $\frac{1}{v(P)}\left(\frac{\partial v}{\partial P}\right)_T$ and γ_T are also calculated at $P = 0$. Similarly, the coefficient C_0 in the Vinet EOS (Eq. (2.7)) can be defined in terms of the γ_T and the frequency shifts by taking the derivative of B_0 (Eq. (2.11)) with respect to the pressure at $P = 0$ as

$$C_0 = \frac{\partial}{\partial P}\left[\gamma_T(P)v(P)(\partial P/\partial v)_T\right] \tag{2.12}$$

We have demonstrated to calculate the coefficients B_0 and C_0 (Eq. (2.7)) spectroscopically by considering nonlinear (quadratic) pressure dependence of the vibrational frequency and the volume according to

$$v(P) = a_1 + b_1P + c_1P^2 \tag{2.13}$$

and

$$V(P) = a_2 + b_2P + c_2P^2 \tag{2.14}$$

where the coefficients (a_1, b_1, c_1 and a_2, b_2, c_2) are constants or in the linear dependence

($c_1 = c_2 = 0$) as the simplest form. By the definition of B_0 and C_0 (at $P = 0$), we find that

$B_0 = -a_2/b_2$ as a constant for both quadratic and linear variations of $v(P)$ and V(P) with the pressure, whereas the coefficient C_0 is obtained as -1 for the linear variations of both V(P) and $v(P)$. In the case of quadratic (nonlinear) dependence of the volume on the pressure, $C_0 = 2a_2c_2/b_2^2$. Regarding the linear and quadratic dependence of the vibrational frequency on the pressure, $v(P)$, the coefficients C_0 can be easily evaluated if the γ_T is independent of pressure, which can be the case for some materials. In this case, $B_0 = \gamma_T(a_1/b_1)$ as a constant at $P = 0$ according to Eq. (2.11) and $C_0 = \gamma_T$ when v varies linearly with the pressure (Eq. (2.13) with c_1=0). If $v(P)$ is quadratic (Eq. (2.13)), then $B_0 = \gamma_T(a_1/b_1)$ as in the linear case, whereas $C_0 = \gamma_T\left(1 - \frac{2a_1c_1}{b_1^2}\right)$ by Eq. (2.12). After all, the P-v relation corresponding to the P-V relation of the Vinet EOS (Eq. (2.7)) can be expressed in terms of the isothermal mode Grüneisen parameter γ_T and the frequency shifts $(\partial v/\partial P)_T$ as

$$P = 3B_0\left[\frac{1-u_v}{u_v^2}\right]exp\left[\frac{3}{2}(C_0-1)(1-u_v)\right] \tag{2.15}$$

with the definitions of u_v (Eq. (2.9)), B_0 (Eq. (2.11)) and C_0 (Eq. (2.12)). Thus, the Vinet EOS for the V-P relation corresponds to the v-P relation (Eq. (2.15)) with the frequency shifts $(\partial v/\partial P)$ (variation of the frequency with the pressure) and the isothermal Grüneisen parameter γ_T (Eq. (2.10)). This is the modification of the Vinet EOS for the spectroscopic parameters. It predicts the vibrational frequency as a function of pressure for various materials.

2.4. Calculation of the thermodynamic quantities

The thermodynamic quantities of the vibrational free energy (F_{vib}), entropy (S), heat capacity (C_V) and enthalpy (H) can be evaluated according to Eqs. (2.1)–(2.4),respectively, at various temperatures from the vibrational frequencies in the quasi-harmonic approximation, as stated above. Their pressure dependence, on the other hand, can also be evaluated from the v-P relation (Eq. (2.15)) as we have derived. Firstly, from the P-V relation (Eq. (2.7)) and the pressure dependence of the vibrational frequency $v(P)$, the mode Grüneisen parameter γ_T can be determined (Eq. (2.10)). Alternatively, by means of the γ_T and V(P), the vibrational frequency $v(P)$ can be evaluated at various pressures at room temperature according to Eq. (2.6). The pressure dependence of the vibrational frequency v(P) then leads to the evaluation of F_{vib}(P), S(P), C_V(P) and H(P) using Eqs. (2.1)–(2.4), respectively, on the basis of the quasi-harmonic approximation. This is done by means of the P-T phase diagram according to the functional form of the T(P) as determined experimentally or evaluated theoretically for various compounds studied. In this study, we calculate the pressure dependence of the thermodynamic quantities of interest from the vibrational frequencies for the cubic gauche nitrogen (cg-N) using the experimental data from the literature.

3. Calculations and results

We first analysed the P-V phase diagram of the cg-N (at $T = 295$ K) by fitting the Vinet EOS (Eq. (2.7)) to the experimental data [5] as shown in Fig. 2. This fitting has been previously performed by using polynomial Murnagan, Burch-Murnagan (BM) and Vinet functions for cg-N($T = 295$ K) [5], as also calculated in an earlier study [4]. Values of the parameters (Eq. (2.7)) from our fit are given in Table 1. Next, the observed Raman frequencies of the ~600 cm^{-1} [3] and ~800 cm^{-1} [24,25] phonon

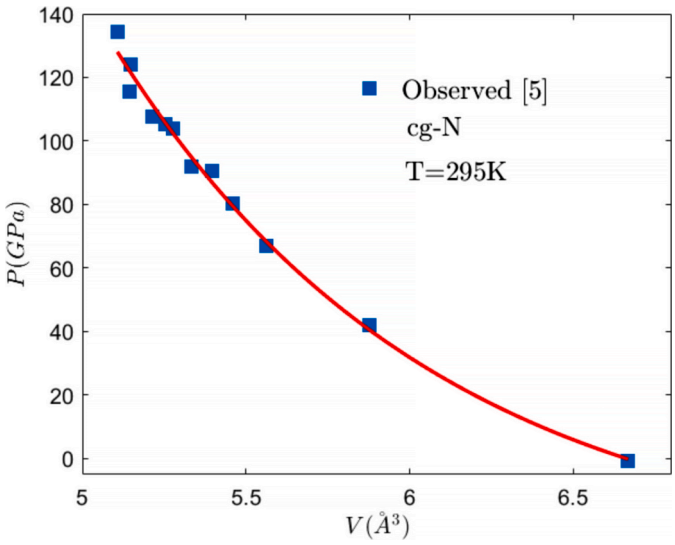

Fig. 2. P-V phase diagram calculated according to the Vinet EOS (Eq. (2.7)) using the experimental data [5] for the cg-N at 295 K.

Table 1
Values of the coefficients using the Vinet EOS (Eq. (2.7)) which was fitted to the experimental data [5] for the cg-N ($T = 295$ K) in comparison with the previous work. Calculated value of V_0 is 6.67 Å^3 [4].

)	B_0(GPa)	$C_0(=B')$	Pressure interval(GPa)	Refs.
6.66	223.13	6.0	0.05<P<134.17	This work
6.6	298	4.0	0<P<100	Ref. [5]

modes which were measured as a function of pressure, were analysed. For the analysis of the vibrational frequencies, we assumed the quadratic dependence of the frequency on the pressure according to Eq. (2.13) although those Raman frequencies varied nearly linearly, as indicated experimentally [24,25]. Values of the coefficients a_1, b_1 and c_1 (Eq. (2.13)) from the fitting procedure, are given in Table 2. Raman frequencies of the phonon modes were evaluated as a function of pressure for the cg-N structure with the observed data for the 600 cm^{-1} [3] and 800 cm^{-1} [24,25] modes according to Eq. (2.13). The pressure dependence of the isothermal mode Grüneisen parameter γ_T was determined by means of Eq. (2.10) using volume [5] and the Raman frequency data for both phonon modes of ~600 cm^{-1} [3] and ~ 800 cm^{-1} [24,25]. We plot γ_T versus P in Fig. 3 for both phonon modes. This led us to predict the Raman frequencies of those modes according to Eq. (2.6) by means of the pressure dependence the γ_T and the volume data [5] for the cg-N,

Table 2
Values of the coefficients for the υ-P relation (Eq. (2.13)) due to the Raman frequencies of the ~600 cm^{-1} [3] and ~800 cm^{-1} [24,25] phonon modes at $T =$ 295 K and for the T-P phase line relation (Eq. (3.1)) within the temperature and pressure intervals indicated [31] for the cg-N structure.

υ -P (Eq. (2.13))	$a_1(=\upsilon_0)$ (cm^{-1})	b_1 (cm^{-1}/GPa)	c_1x10^{-3} (cm^{-1}/GPa^2)	Pressure Interval (GPa)
υ (600 cm^{-1})	618.12	2.67	−6.4	24.05<P<151.70
υ (800 cm^{-1})	711.14	1.02	0.9	24.05<P<151.70
T-P relation (Eq. (3.1))	-a(K) x10^3	b (K/GPa)	-c (K/GPa^2)	T(K) -P(GPa) Interval
[31]	18.51	231.72	0.47	31.85<T<2046.18 103.9<P<116.90
[32]	66.81	46.36	143.39	1066.37<T<3840.71 26.45<P<149.98

as plotted in Fig. 4. υ_0 values of the Raman frequencies according to Eq. (2.13) at $P = 0$, are also given in Table 2.

Two Raman active modes of A (~600 cm^{-1}) and T (~800 cm^{-1}) were chosen in our treatment to calculate their frequencies. By means of those frequencies, the pressure dependence of the thermodynamic properties were predicted using the quasi-harmonic approximation for the cg-N structure.

As we calculated the pressure dependence of the mode Grüneisen parameter γ_T for the A and T modes (Fig. 3) at room temperature for the cg-N structure, which diverge close to the phase transition ($P_c \cong 140$ GPa), we find that their calculated Raman frequencies also diverges (Fig. 4). However, experimentally, there is no any divergence behaviour of those two Raman modes at around 140 GPa. Due to the anomalous behaviour of the A and T modes close to ~140 GPa, those two modes were particularly chosen to predict the thermodynamic properties in the cg-N structure.

In order to evaluate the pressure dependence of the thermodynamic quantities of the free energy (F_{vib}), entropy (S), heat capacity (C_V) and enthalpy (H) according to Eqs. (2.1)–(2.4), respectively, contributions due to the vibrational frequencies of the ~600 cm^{-1} [3] and ~ 800 cm^{-1} [24,25] Raman modes were considered. Those thermodynamic quantities were calculated from the vibrational frequencies for each mode separately as a function of pressure. Since Eqs. (2.1)–(2.4) provide the temperature dependence of F_{vib}, S, C_V and H, respectively, we used the T-P dependence for the cg-N, which was predicted previously [31,32], as stated above. The T-P dependence was considered in the quadratic form within the temperature and pressure intervals which we studied for the cg-N as

$$T(P) = a + bP + cP^2 \tag{3.1}$$

where a,b and c are all constants. From the predicted T-P values for the cg-N [31,32], we determined the coefficients according to Eq. (3.1) as given in Table 2. This T-P dependence is plotted in Fig. 5 for the cg-N melting. Then, by using Eq. (3.1) in Eqs. (2.1)–(2.4) for the Raman frequencies of the ~600 cm^{-1} [3] and ~ 800 cm^{-1} [24,25] modes, we calculated the pressure dependence of the of F_{vib} (Fig. 6a), S (Fig. 7a), C_V (Fig. 8a) and H (Fig. 9a). These plots therefore represent our predictions of the thermodynamic quantities studied due to the contributions of the vibrational frequencies (~600 cm^{-1} and ~ 800 cm^{-1}) within the quasi-harmonic approximation at various pressures for the cg-N structure.

Additionally in this study, we also considered contributions of the other Raman modes to the thermodynamic properties of the cg-N structure. Those Raman modes are 1xRaman, 2xRaman and 3xRaman [7], A, E, T(TO) and T(LO) modes [13]. B_{2g} and B_{3g} [16] modes. The pressure dependence of F_{vib} is calculated according to Eq. (2.1) due to~600 cm^{-1} and ~ 800 cm^{-1} Raman modes (Fig. 5a). Fig. 5b gives the variation of F_{vib} with the pressure due to the A,E, T(TO) and T(LO) modes. Contributions to the vibrational energy due to the 1xRaman, 2xRaman and 3xRaman (Fig. 6c) and, the Raman modes]. B_{2g} and B_{3g} (Fig. 6d) were also calculated.

In the same order, contributions to the entropy S according to (Eq. (2.2)) due to the Raman modes studied, are plotted in Fig. 7 (a,b,c,d) contributions to the heat capacity C_V (Eq. (2.3)) in Fig. 8 (a–d) and to the enthalpy H (Eq. (2.4)) in Fig. 9 (a–d). Thus, we were able to calculate vibrational energy F_{vib}, S, C_V and H due to the all Raman modes considered in this study.

4. Discussion

The vibrational frequencies of the Raman modes (~600 cm^{-1} and ~ 800 cm^{-1}) were predicted (Eq. (2.6)) from the volume data [5] by determining the isothermal mode Grüneisen parameter γ_T (Eq. (2.5)) using the observed frequencies of the 600 cm^{-1} [3] and 800 cm^{-1} [24, 25] modes for the cg-N structure, as stated above. For this prediction, the

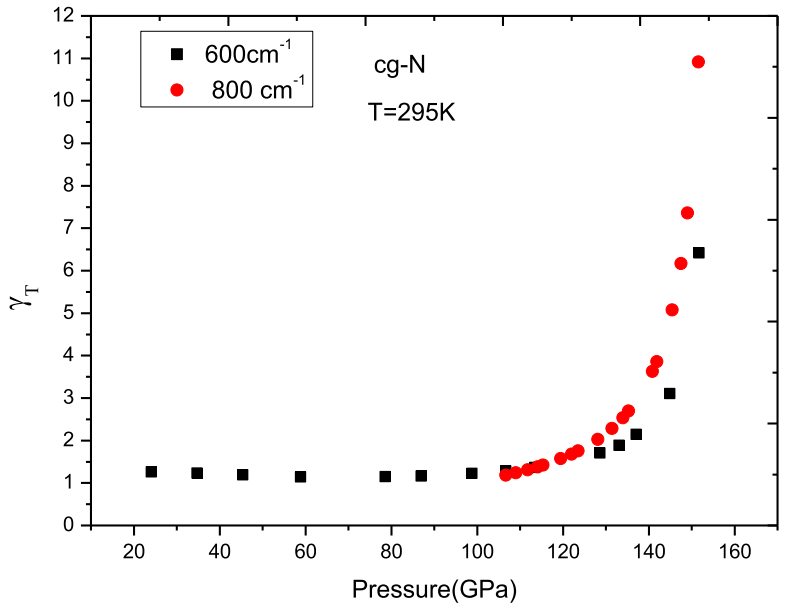

Fig. 3. Pressure dependence of the mode Grüneisen parameter γ_T using the experimental data for the volume [5] and, for the 600 cm^{-1} [3] and 800 cm^{-1} [24,25] Raman modes of the cg-N at $T = 295$ K.

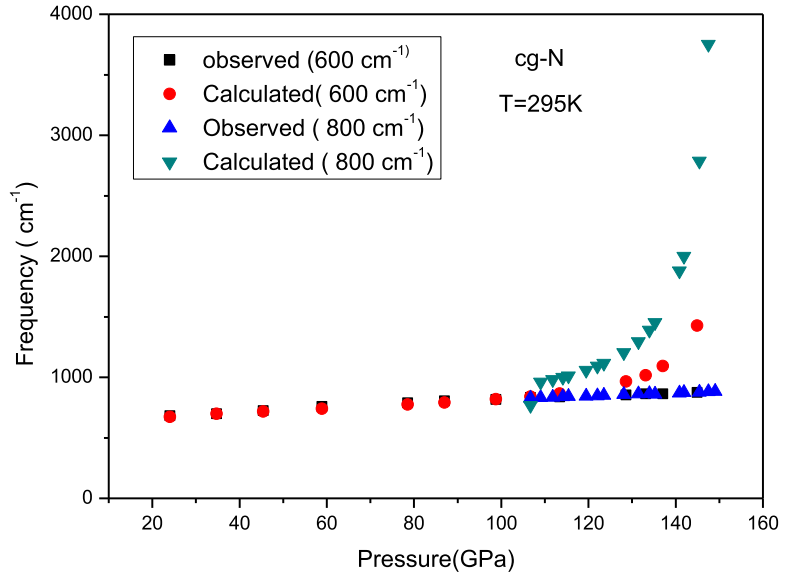

Fig. 4. Pressure dependence of the Raman frequencies calculated according to Eq. (2.6) using the observed volume data [5] and the γ_T values (Fig. 2) for the cg-N at $T = 295$ K.

Vinet EOS (Eq. (2.7)) was fitted to the P-V data [5], which describes the observed behaviour satisfactorily ($T = 295$ K) for the cg-N, as shown in Fig. 1. This is almost the same plot as obtained previously by using the Burch-Murnagan (BM)-EOS [5].

Regarding the pressure dependence of the γ_T of both Raman modes as we evaluated (Fig. 2), their γ_T values do not vary with the pressure (up to$\sim$ 100 GPa) $\gamma_T \cong 1$, at low pressures. Above about 110 GPa, the γ_T values of both Raman modes vary considerably with the pressure and the γ_T grows largely at $\sim$ 150 GPa (Fig. 2) as we also obtained in our previous study [20]. This causes divergence behaviour of the Raman frequencies of the 600 cm^{-1} and 800 cm^{-1} modes, in particular, it is shown by the 800 cm^{-1} mode which we predicted according to Eq. (2.6). However, the observed frequencies of the 600 cm^{-1} [3] and 800 cm^{-1} [24,25] modes are nearly independent of the pressure, as shown in Fig. 4. The Raman modes of A ($\sim$ 600 cm^{-1}) and T (800 cm^{-1}) appear experimentally at the pressures between nearly 20 and 150 GPa, as shown in Fig. 3. Note that there is no any phase transition observed experimentally above about 100 GPa due to those two Raman modes (A and T modes), as shown in Fig. 4. However, as a result of the divergence behaviour of the mode Grüneisen parameter γ_T of the A and T modes above 100 GPa (Fig. 3), there also occurs divergence of the Raman frequencies of those modes as predicted according to Eq. (2.6). On the basis of our predicted Raman frequencies of the A and T modes, it can be argued that a phase transition occurs at about 140 GPa in the cg-N structure [33]. Since we modified the Vinet EOS (Eq. (2.7)) for the spectroscopic parameters as the υ-P relation (Eq. (2.15)), the vibrational frequencies of the 600 cm^{-1} and 800 cm^{-1} Raman modes and also the other Raman modes studied can be predicted from this relation for the cg-N structure. Thus, the volume jump (ΔV) for the V-P relation corresponds to the change in the frequency jump ($\Delta\ \upsilon$) in the υ-P relation

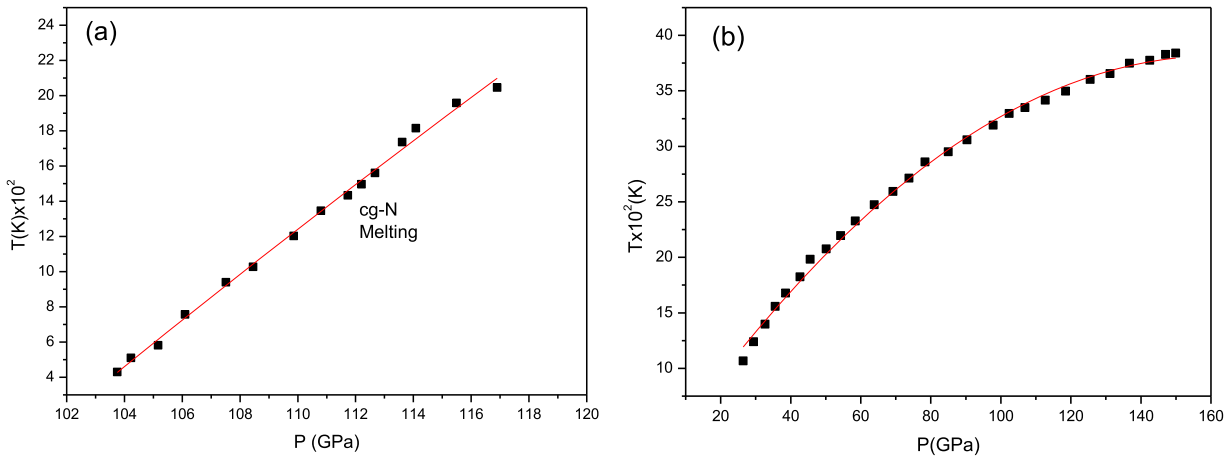

Fig. 5. T-P phase diagram for the cg-N melting which was predicted (a) [31], as also given previously [18] and (b) [32] according to Eq. (3.1) within the temperature and pressure intervals (Table 2).

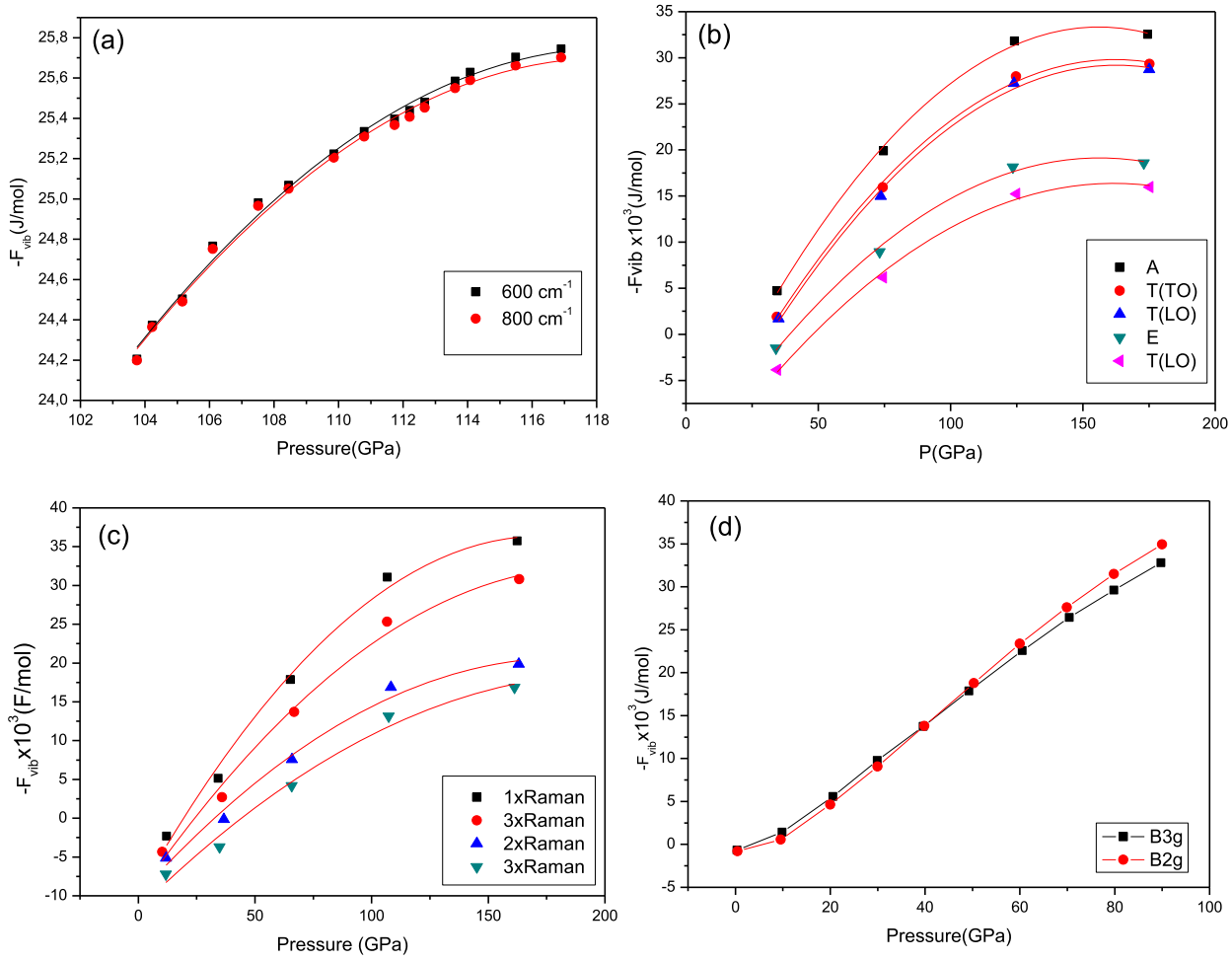

Fig. 6. Pressure dependence of the free energy F_{vib} predicted by the quasi-harmonic theory (Eq. (2.1)) using the Raman modes indicated for the cg-N($T = 295$ K).

during the cg-N transition. By means of the mode Grüneisen parameter (γ_T), they are correlated with each other. This can also apply to some other vibrational frequencies as predicted from the observed frequencies with the mode Grüneisen parameter (γ_T) at various pressures. From the experiments point of view, the spectroscopic parameters, mainly the frequency shifts, at various pressures, $(\partial\upsilon/\partial P)$ can be measured to high accuracy as compared to the volume changes. By determining the mode Grüneisen parameter (γ_T), spectroscopic parameters (frequency shifts) can be predicted by the modified expression (Eq. (2.15)) of the Vinet EOS for various materials.

Note that as a demonstration, we assumed the quadratic dependence of the volume on the pressure (Eq. (2.14)) in order to determine B_0 and C_0 in Eq. (2.15). Thus, in the simplest form (linear or quadratic) of $\upsilon(P)$ and V(P), as given by Eqs. (2.13) and (2.14), respectively, we were able

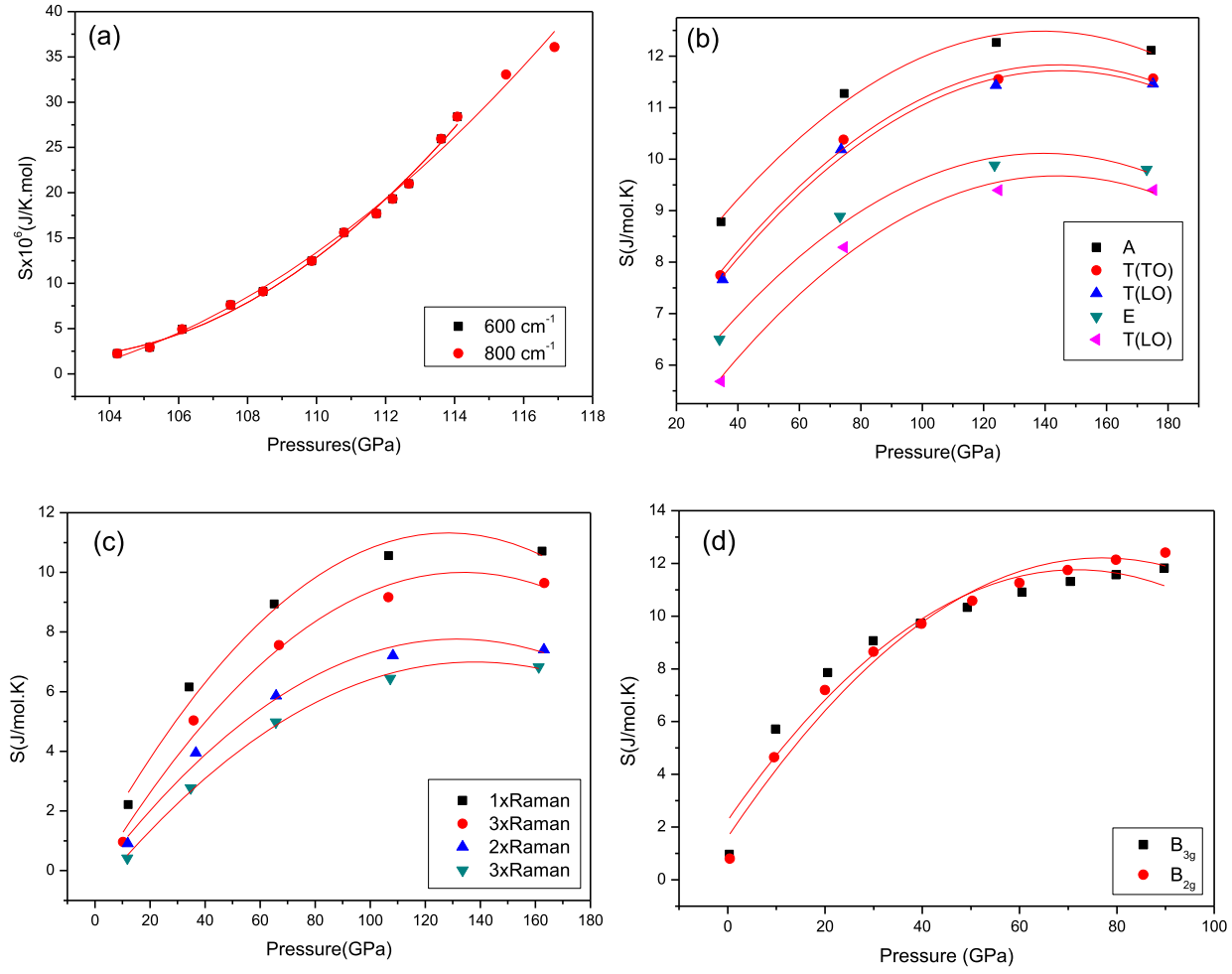

Fig. 7. Pressure dependence of the entropy S predicted by the quasi-harmonic theory (Eq. (2.2)) using the Raman modes indicated for the cg-N(T = 295 K).

to define B_0 and C_0 .

It is obvious that the volume depends upon the pressure according to the Vinet EOS (Eq. (2.7)) in general. Correspondingly, the vibrational frequency can depend on the pressure by the P- v relation (Eq. (2.15)) which is spectroscopically equivalent to the P-V relation (Eq. (2.7)). However, when we analysed the Raman frequencies of the ~ 600 cm^{-1} and 800 cm^{-1} modes, we used for simplicity the quadratic pressure dependence according to Eq. (2.13). At high pressures up to ~110 GPa, quadratic pressure dependence of the vibrational frequencies (600 cm^{-1} and 800 cm^{-1}) (Eq. (2.13)) satisfies the observed data. However, just above ~110 GPa, Eq. (2.13) does not describe the observed behaviour of those Raman frequencies which diverges particularly, 800 cm^{-1}mode frequencies (Fig. 4) due to the fact that the γ_T diverge in this pressure region (Fig. 3) for the cg-N structure as studied above. In our treatment given here, we analysed the experimental V-P data [5] and we used the Vinet EOS (Eq. (2.7)) which is not quadratic.

Using the quasi-harmonic approximation, the thermodynamic quantities of the free energy (F_{vib}), entropy (S), heat capacity (C_V) and enthalpy (H) which were predicted, decrease as shown by Fig. 5 (F_{vib}) and (Fig. 6a (S) whereas S (Fig. 6) and H (Fig. 8) increases with the pressure for the cg-N structure. This is the expected behaviour of those functions as also evaluated in some earlier studies. As obtained from the first principle calculations, the negative free energy decreases with the increasing temperature up to 2000 K [12] and it increases with the pressure (up to 600 GPa) [11] as we obtained in this study for the cg-N structure. Increasing behaviour of the energy with the pressure was also obtained for the cg-N structure as reported in an earlier study [32], which also confirms our result in this study. Also, the calculated Helmholtz free energy (negative F) decreases monotonously with the increasing temperature in $AgGeS_2$ at zero pressure as indicated previously [29]. Regarding the temperature and pressure dependence of the entropy (S), heat capacity (C_V) and enthalpy(H), those thermodynamics quantities increase with increasing temperature. This is shown for the temperature dependence of S(T), H(T) and C_V(T) [3] for the cg-N. Increasing behaviour of S(T), H(T) and C_V(T) with the temperature has also been obtained for $AgGeS_2$ [29]. The first principle calculations show that the enthalpy (H) increases as the pressure increases at low pressures (up to 60 GPa) [15] and also at high pressures between 100 and 400 GPa [34] for the cg-N, which also agrees with our prediction of the enthalpy H by the quasi-harmonic approximation as given here. Additionally, using ab initio calculations based on density-functional theory, the enthalpy difference (H—H_{cg}) has been calculated up to 360 GPa (at 0 K), which does not vary with the pressure. i.e. the enthalpy (H—H_{cg}) increases with the pressure [17]. Our prediction for the H_{cg} also is in agreement with this previous study.

Our calculations of the Helmholtz free energy (F_{vib}) which decreases, give almost the same values due to the 600 cm^{-1} and 800 cm^{-1} Raman modes (Fig. 6a), and for the B_{2g} and B_{3g} Raman modes (Fig. 6d) as a function of pressure for the cg-N structure whereas for the other Raman modes studied, the free energy increases smoothly with the pressure as shown in Fig. 6b and c. For the entropy S which increases with the pressure, calculated values are also the same for the Raman modes of 600 cm^{-1} and 800 cm^{-1} (Fig. 7a). However, they are all different for the other Raman modes (Fig. 6b–d). The entropy S increases from the T(LO)

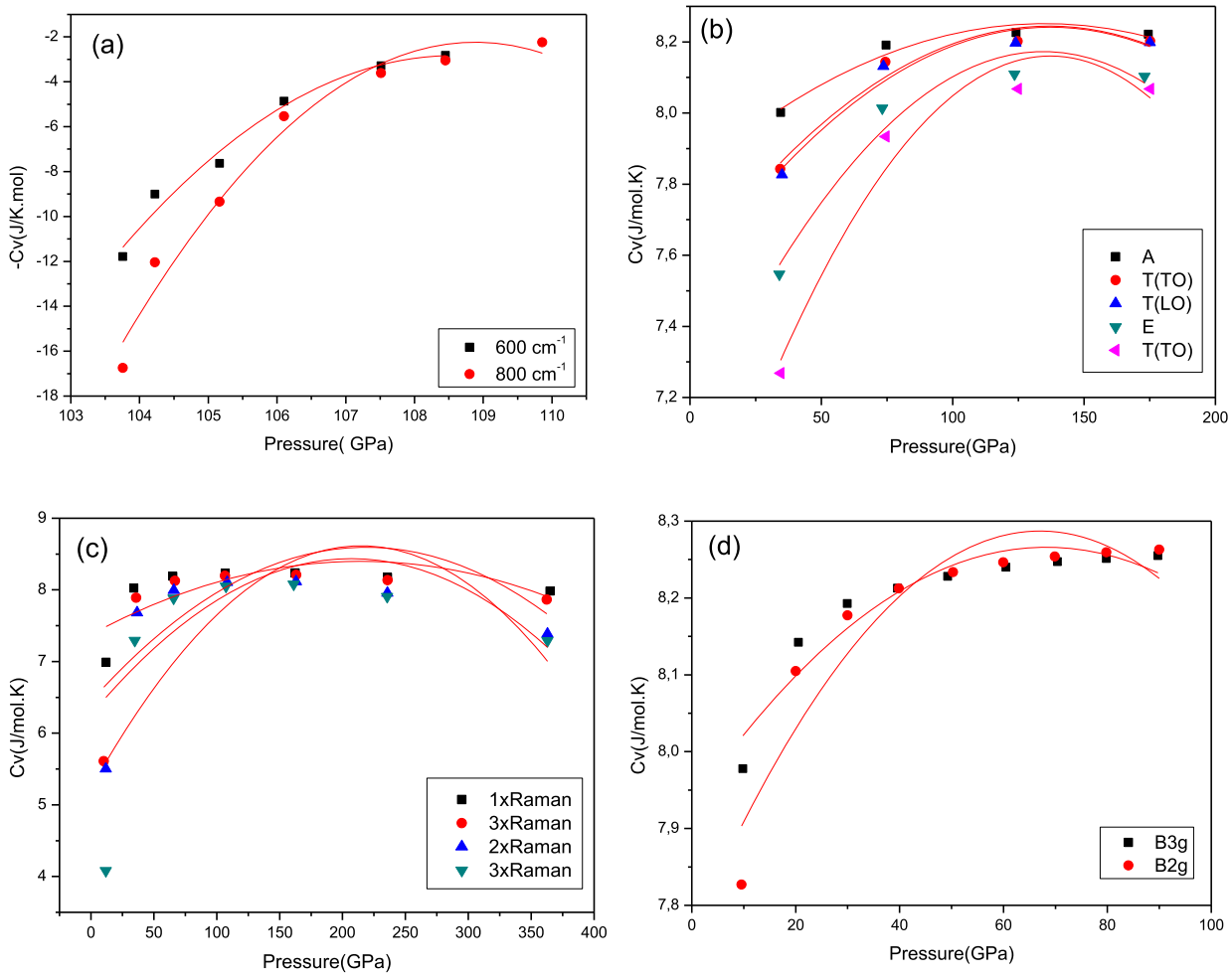

Fig. 8. Pressure dependence of the specific heat C_V predicted by the quasi-harmonic theory (Eq. (2.3)) using the Raman modes indicated for the cg-N(T = 295 K).

to the A Raman modes (Fig. 7b) as the F_{vib}((Fig. 6b). It also increases in magnitude from the 3xRaman to 1xRaman mode (Fig. 7c) similar to the F_{vib}(Fig. 5c). This increase also occurs from B_{2g} to B_{3g} (Fig. 7d) compared to the F_{vib} (Fig. 7d). Thus, this increasing of the entropy (S) and the free energy F_{vib} with the increasing pressure, occurs for all the Raman modes studied here, as expected. For the C_V(P) and H(P) behaviour is rather different as shown in Figs. 8 and 9, respectively, C_V decreases with the pressure, contributions to the negative C_V due to the 800 cm^{-1} Raman mode seem to be larger than the 600 cm^{-1} mode and their contribution is almost the same above about 106 GPa within the pressure region of 103–110 GPa (Fig. 8a).For the Raman modes of A, T(TO), T(LO)and E, the heat capacity C_v increases with the pressure (Fig. 8b) as the free energy F_{vib} (Fig. 6b) and the entropy (Fig. 7b). This increase of C_v also occurs due to the other Raman modes (Fig. 8c,d). The situation is completely different for the pressure dependence of the enthalpy H(P) due to the contributions of the Raman modes 600 cm^{-1} and 800 cm^{-1}, as shown in Fig. 9a. Contribution to the H due to the 800 cm^{-1} Raman mode is constant (~5.2 × 10^3 J/mol), whereas contribution due to the 800 cm^{-1} mode increases from the 4.2 × 10^3J/mol to the constant value indicated. In the same pressure region as in the C_V (103-110 GPa), the entropy H increases with the increasing pressure (Fig. 9a). This increase of H also occurs for the other Raman modes studied here (Fig. 9b–d). Differently from the behaviour of F_{vib} (Fig. 6b), S (Fig. 7b) and C_v (Fig. 8b), we obtained a single curve of H for the all Raman modes fo A, T (TO), T(LO) and E, which increases with the pressure as shown in Fig. 9b. The enthalpy also increases with the pressure as in the same sense of F_{vib} (Fig. 6c,d), S (Fig. 7c,d) and C_v (Fig. 8c,d) contributions due to the Raman modes studied, as plotted in Fig. 9c,d.

It has been indicated that diatomic phase occurring at low pressures transforms into the single-bonded (polymeric) phase(cg-N) as a first order transition at high pressures [4]. Divergence behaviour of the γ_T (Fig. 3) and the Raman frequencies of the 600 cm^{-1} and 800 cm^{-1} modes (Fig. 4) above 140 GPa, which are almost the pressure-independent at low pressures (below about 100 GPa), also exhibits the existence of the cg-N structure at high pressures. This is supported by the increasing thermodynamic properties with the increasing pressure above ~ 100 GPa namely, the free energy (Fig. 6), entropy (Fig. 7), heat capacity (Fig. 8) and the enthalpy (Fig. 9). At high pressures (above ~ 100 GPa, they also confirm the existence of the cg-N structure so that the single-bonded (polymeric) phase occurs, as predicted by the quasi-harmonic approximation. With this large energy at high pressures, the cg-N structure is considered a high energy capacity material [4,35] which transforms into highly stable molecular states with a large release of energy [36]. Thus, jumps in the Raman frequencies of the 600 cm^{-1} and 800 cm^{-1} modes as examples, at the high pressure (about 140 GPa) indicate a first order transition from the molecular nitrogen to the cubic-gauche structure, which gives rise to the increasing of the thermodynamic properties with the pressure, as stated above. Therefore, we can conclude that the Raman active modes studied here play an important role in the mechanism of the phase transition for the cg-N structure.

In this study, the thermodynamic properties of the cg-N structure were predicted by the quasi-harmonic approximation. Regarding density-functional perturbation theory [11,13,16] and the linear

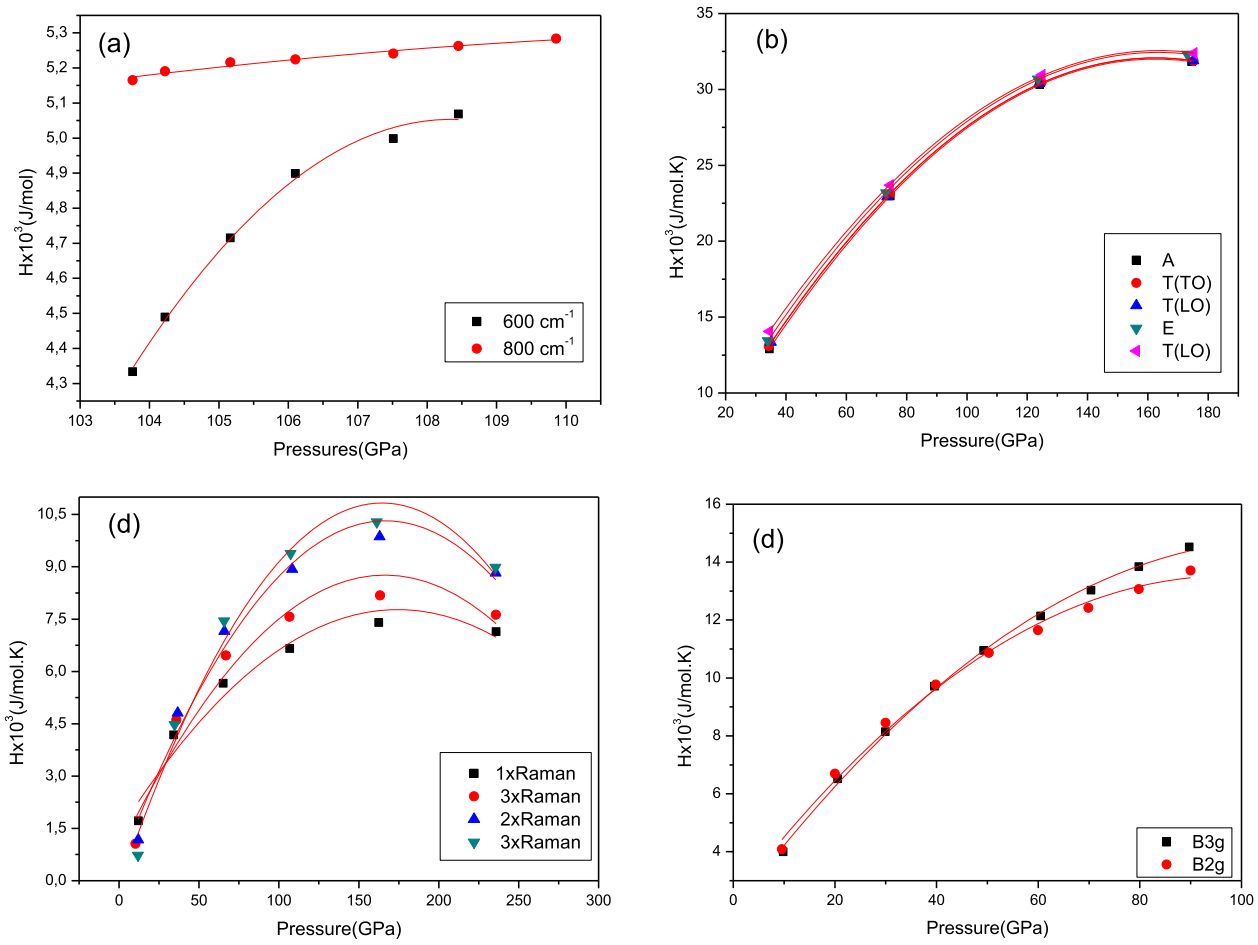

Fig. 9. Pressure dependence of the enthalpy H predicted by the quasi-harmonic theory (Eq. (2.4)) using the Raman modes indicated for the cg-N(T = 295 K).

response theory [7], both theories required to calculate the phonon dispersion throughout the Brillouin zone. i.e. the phonon density of states over the whole frequency range is integrated, as stated above. The thermodynamic properties were then predicted for the cg-N in the earlies studies. The combination of the density functional theory and quasi-harmonic approximation can also predict the thermodynamic properties of the materials. In our treatment, we considered the frequencies of the Raman-active modes which contribute to the thermodynamic properties. Then, a sum of those frequencies was used to predict the pressure dependence of the thermodynamic quantities by the quasi-harmonic approximation. From this point of view, our predictions of the thermodynamic properties should give similar behaviour qualitatively as those predicted by the density functional theory. Quantitatively, in terms of computational accuracy, density functional theory can give better results because of the whole frequency range integrated to evaluate the thermodynamic properties.

Prediction of the thermodynamic properties such as free energy, entropy, heat capacity and enthalpy was conducted in the present study for the cubic gauche nitrogen, as we have partly studied in our earlier works [19,20] .For those predictions, we used the quasi-harmonic theory in this study as stated above. Differently from our previous studies, we also concentrated here to derive the frequency-pressure (υ-P) relation corresponding to the Vinet EOS (V-P relation) for the spectroscopic parameters, mainly for the cg-N structure. As indicated previously, the υ-P relation introduced in this study, provides to the predicting the frequency as a function of pressure by means of the mode Grüneisen parameter for various crystalline materials. From the accurate measurements of the vibrational frequencies as a function of pressure, our υ-P relation (Eq. (2.15)) can be employed with the mode Grüneisen parameter (γ_T) to the predict the frequencies throughout the Brillouin zone for various crystalline materials.

5. Conclusions

The Raman frequencies of the ~600 cm^{-1} and ~800 cm^{-1} modes were calculated at various pressures (T = 295 K) from the volume data through the mode Grüneisen parameter γ_T for the cg-N structure. Our results give the anomalous behaviour of the γ_T and the Raman frequencies of those modes. The Vinet EOS (V-P) was reformulated as the frequency-pressure (υ -P) relation for the spectroscopic parameters of the crystalline structures. Using the quasi-harmonic approximation, the thermodynamic quantities were predicted, and their pressure dependence was obtained from the Raman frequencies of various modes which contribute to those thermodynamic properties for the cg-N transition.

Those thermodynamic functions studied, increase with the pressure, as expected for the cg-N structure. This indicates that the quasi-harmonic approximation is adequate at high pressures for the cg-N transition.

Declaration of Competing Interest

The authors declare that they have no known competing financial interests or personal relationships that could have appeared to influence the work reported in this paper.

Data availability

No data was used for the research described in the article.

References

[1] A.K. McMahan, R. Lesar, Pressure dissociation of solid nitrogen under 1 Mbar, Phys. Rev. Lett 54 (1985) 1929.
[2] C. Mailhiot, L.H. Yang, A.K. McMahan, Polymeric nitrogen, Phys. Rev. B 46 (1992) 14419.
[3] M.I. Eremets, A.G. Gavriliuk, I.A. Trojan, D.A. Dzivenko, R. Boehler, Single-bonded cubic form of nitrogen, Nat. Mater. 3 (2004) 558.
[4] M.I. Eremets, A.G. Gavriliuk, N.R. Serebryanaya, I.A. Trojan, D.A. Dzivenko, R. Boehler, H.K. Mao, R.J. Hemley, Structural transformation of molecular nitrogen to a single-bonded atomic state at high pressures,, J. Chem. Phys. 121 (2004) 11296.
[5] M.I. Eremets, A.G. Gavriliuk, I.A. Trojan, Single-crystalline polymeric nitrogen, Appl. Phys. Lett. 90 (2007) 171904.
[6] R.M. Martin, R. Needs, Theoretical study of the molecular-to-nonmolecular transformation of nitrogen at high pressures, Phys. Rev. B 34 (1986) 5082.
[7] T.W. Barbee III, Metastability of atomic phases of nitrogen, Phys. Rev. B 48 (1993) 9327.
[8] M.M.G. Alemany, J.L. Martins, Density-functional study of nonmolecular phases of nitrogen: metastable phase at low pressure, Phys. Rev. B 68 (2003), 024110.
[9] W.D. Mattson, D. Sanchez-Portal, S. Chiesa, R.M. Martin, Prediction of new phases of nitrogen at high pressure from first-principles simulations, Phys. Rev. Lett. 93 (2004) 125501.
[10] L.N. Yakub, Thermodynamics of solid polymerized nitrogen, J. Low Temp. Phys. 139 (2005) 783.
[11] H.L. Yu, G.W. Yang, X.H. Yan, Y. Xiao, Y.L. Mao, Y.R. Yang, M.X. Cheng, First-principles calculations of the single-bonded cubic phase of nitrogen, Phys. Rev. B 73 (2006), 012101.
[12] H.L. Yu, G.W. Yang, X.H. Yan, Y. Xiao, Y.L. Mao, Y.R. Yang, Y. Zhang, Lattice dynamics of single-bonded cubic nitrogen, Chem. Phys. Lett. 417 (2006) 272.
[13] R. Caracas, Raman spectra and lattice dynamics of cubic gauche nitrogen, J. Chem. Phys. 127 (2007) 144510.
[14] J. Zhao, First-principles study of atomic nitrogen solid with cubic gauche structure, Phys. Lett. A 360 (2007) 645.
[15] F. Zahariev, J. Hooper, S. Alavi, F. Zhang, T.K. Woo, Low-pressure metastable phase of single-bonded polymeric nitrogen from a helical structure motif and first-principles calculations, Phys. Rev. B 75 (2007) 140101.
[16] R. Caracas, R.J. Hemley, New structures of dense nitrogen: Pathways to the polymeric phase, Chem. Phys. Lett. 442 (2007) 65.
[17] X. Wang, F. Tian, L. Wang, T. Cui, B. Liu, G. Zou, Structural stability of polymeric nitrogen: A first-principles investigation, J. Chem. Phys. 132 (2010), 024502.
[18] L.N. Yakub, Phase transition line of solid molecular nitrogen into the cubic gauche-polymeric phaseLow Temp. Phys. 37 (2011) 431.
[19] H. Yurtseven, O. Tiryaki, O. Tari, Pippard relations for cubic gauche nitrogen, Anadolu Univ. J. Sci. Technol. Appl. Sci. Eng. 17 (2016) 741.
[20] O. Akay, H. Yurtseven, Investigation of vibrational, elastic and dielectric properties of cubic gauche nitrogen (cg-N),, Optik 236 (2021) 166481.
[21] M.I. Eremets, R.J. Hemley, H.K. Mao, E. Gregoryanz, Semiconducting non-molecular nitrogen up to 240 GPa and its low-pressure stability, Nature 411 (2001) 170.
[22] E. Gregoryanz, A.F. Goncharov, R.J. Hemley, H. Mao, High-pressure amorphous nitrogen, Phys. Rev. B 64 (2001), 052103.
[23] M.J. Lipp, J.P. Klepeis, B.J. Baer, H. Cynn, W.J. Evans, V. Iota, C.S. Yoo, Transformation of molecular nitrogen to nonmolecular phases at megabar pressures by direct laser heating, Phys. Rev. B 76 (2007), 014113.
[24] M. Pa, S. Liu, L. Lei, F. Zhang, L. Feng, L. Qi, L. Zhang, Raman study of pressure-induced dissociative transitions in nitrogen, Solid State Commun. 298 (2019) 113645.
[25] L. Lei, Q.Q. Tang, F. Zhang, S. Liu, B.B. Wu, C. Zhou, Evidence for a new extended solid of nitrogen, Chin. Phys. Lett. 37 (2020), 068101.
[26] P. Vinet, J. Ferrante, J.R. Smith, J.H. Ross, A universal equation of state for solids, J. Phys. C 19 (1986) 467.
[27] A.A. Maradudin, E.W. Montroll, G.H. Weiss, Theory of Lattice Dynamics in the Harmonic Approximation, Academic, New York, 1963.
[28] X. Gonze, G.M. Kignanese, R. Caracas, Z. Kristallogr, First-principle studies of the lattice dynamics of crystals, and related properties 220 (2005) 458.
[29] J. Yang, Q. Fan, Y. Yu, W. Zhang, Pressure Effect of the vibrational and thermodynamic properties of chalcopyrite-type compound $AgGaS_2$: A first-principles investigation, Materials 11 (2018) 2370.
[30] H. Yurtseven, H. Özdemir, Temperature dependence of the entropy and the heat capacity calculated from the raman frequency shifts for solid benzene, naphthalene and anthracene, Int. J. Thermodyn. 25 (2022), 055.
[31] A.F. Goncharov, J.C. Crowhurst, V.V. Struzhkin, R.J. Hemley, Triple point on the melting curve and polymorphism of nitrogen at high pressure, Phys. Rev. Lett. 101 (2008), 095502.
[32] H. Alkhaldi, P. Kroll, Chemical potential of nitrogen at high pressure and high temperature: application to nitrogen and nitrogen-rich phase diagram calculations, J. Phys. Chem. C 123 (2019) 7054.
[33] M. Ross, F. Roger, Polymerization, shock cooling, and the high-pressure phase diagram of nitrogen, Phys. Rev. B 74 (2006), 024103.
[34] Y. Ma, A.R. Oganov, Z. Li, Y. Xie, J. Kotakoski, Novel high pressure structures of polymeric nitrogen, Phys. Rev. Lett. 102 (2009), 065501.
[35] X.Q. Chen, C.L. Fu, R. Podloucky, Bonding and strength of solid nitrogen in the cubic gauche (cg-N) structure, Phys. Rev. 77 (2008), 064103.
[36] J. Uddin, V. Barone, G.E. Scuseria, Energy storage capacity of polymeric nitrogen, Mol. Phys. 104 (2006) 745.